

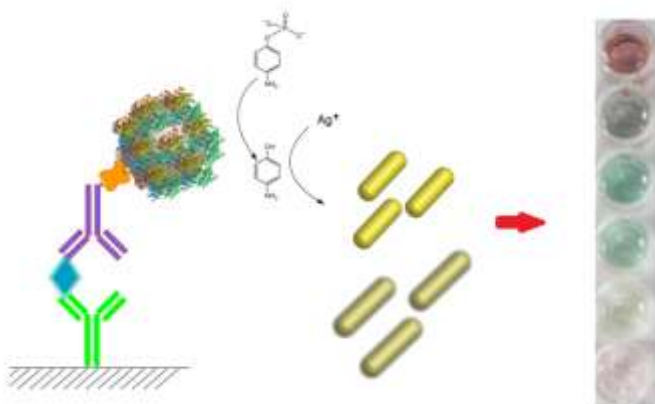


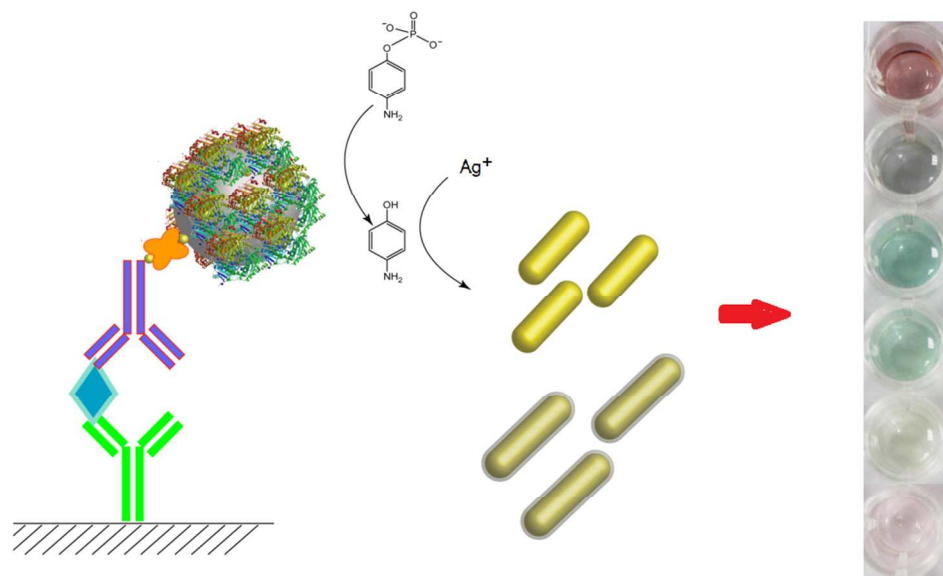
**Enzyme-catalysed deposition of ultrathin silver shells on gold nanorods: A universal and highly efficient signal amplification strategy for translating immunoassay into litmus-type test**

Journal:	<i>ChemComm</i>
Manuscript ID:	CC-COM-02-2015-001286.R1
Article Type:	Communication
Date Submitted by the Author:	10-Mar-2015
Complete List of Authors:	Yang, Xinjian; National University of Singapore, Chemistry Gao, Zhiqiang; National University of Singapore , Chemistry

## Table of Content

A universal and highly efficient signal amplification strategy for uses in protein assays is presented in this communication.





TOC  
246x149mm (120 x 120 DPI)

## COMMUNICATION

## Enzyme-catalysed deposition of ultrathin silver shells on gold nanorods: A universal and highly efficient signal amplification strategy for translating immunoassay into litmus-type test

Cite this: DOI: 10.1039/x0xx00000x

Received 00th January 2012,

Accepted 00th January 2012

DOI: 10.1039/x0xx00000x

[www.rsc.org/](http://www.rsc.org/)

Xinjian Yang and Zhiqiang Gao\*

**On the basis of enzyme-catalysed reduction of silver ions and consequent deposition of ultrathin silver shells on gold nanorods, a highly efficient signal amplification method for immunoassay is developed. For a model analyte prostate-specific antigen, a 10<sup>4</sup>-fold improvement over conventional enzyme-linked immunosorbent assay is accomplished by leveraging on the cumulative nature of the enzymatic reaction and sensitive response of plasmonic gold nanorods to the deposition the silver shells.**

Identification and quantification of protein biomarkers with high sensitivity in complex biological samples are of great significance to clinical decision-making. Highly sensitive and selective detection of protein biomarkers greatly facilitates early-stage and recurrence diagnosis, monitoring disease progression and evaluating therapeutic interventions.[1] Currently, enzymatic amplification techniques have been extensively used in standard antibody-based protein biomarker detections - enzyme-linked immunosorbent assay (ELISA).[2] The biggest advantage of ELISA is its superior selectivity arising from high specificity of antigen-antibody interaction. However, its moderate sensitivity presents a significant challenge when analysing ultralow levels of proteins. The detection limit of most ELISA is ~0.10 ng/ml, which is inadequate to reach the clinical threshold of many protein biomarkers especially in the early stage of diseases. For example, prostate-specific antigen (PSA), produced by prostate gland and other organs such as liver and kidney, is a well-established tumour marker for prostate cancer and breast cancer - the most common types of cancer and the leading cause of cancer death among men and women, respectively.[3] PSA is present at very low levels in the blood of healthy individuals, but is often elevated in the presence of prostate cancer or breast cancer. For example, it has been shown that ultralow levels of PSA in women are closely

associated with breast cancer, a highly sensitive and selective PSA assay for analysis of women's sera must have a detection limit lower than 1 pg/mL,[4] which is difficult to achieve by established assays, thus limiting the use of PSA for breast cancer diagnosis.

Plasmonic metal nanomaterials, which possess extraordinary capabilities for the applications in a wide range of fields, such as chemical sensing and biosensing, photovoltaics, photo-assisted chemical reactions and optical nanoantennas, have attracted great attention over the past decade.[5] Particularly, their ultrahigh extinction coefficients of the surface plasmon resonance (SPR) absorption have offered excellent opportunities for the construction of devices and assays with unparalleled functionalities for highly sensitive detection of a wide range of analytes.[6] Furthermore, the plasmonic properties of these nanomaterials are strongly dependent on their structural parameters such as size, shape, composition, as well as local dielectric environment.[7] These nanomaterials are a group of desirable building blocks for the construction of bioassays and fabrication of biosensors where their plasmonic properties alter in response to biorecognition events. In addition, plasmonic nanomaterials could also act as transducers that convert small changes in the local refractive index into significant spectral shifts in their UV-visible spectra. For instance, gold nanorods (AuNRs) with well-defined and controllable shapes and aspect ratios have attracted extensive attention in recent years because of their unique shape-dependent optical properties.[8] By exploiting the excellent optical properties of the AuNRs, several of nanodevices and SPR biosensors have been constructed.[9] However, most of the gold nanorod-based SPR biosensors suffer from low sensitivity. Herein, we proposed a universal signal amplification method involving the use of alkaline phosphatase and the AuNRs. The proof-of-principle experiments clearly demonstrated that the analytical signal can be significantly amplified through enzyme-catalysed modulation of the local

dielectric environment of the AuNRs, thus providing a universal signal amplification strategy for ELISA and other immunoassays.

As schematically illustrated in Figure 1, this strategy relies on the growth of ultrathin silver shells on the AuNRs in the presence of silver ions and p-aminophenol produced by alkaline phosphatase-catalysed de-phosphorylation of p-aminophenol phosphate. As in conventional ELISA, alkaline phosphatase is brought in through immunoreaction with a target antigen (PSA in this case). With the addition of p-aminophenol phosphate, p-aminophenol is produced by dephosphorylating p-aminophenol phosphate catalysed by alkaline phosphatase. Consequently, silver ions are reduced to metallic silver by p-aminophenol, thus resulting in the deposition of silver on the surface of the AuNRs. Alkaline phosphatase is a hydrolytic enzyme that is extensively used in ELISA due to its high catalytic activity, ease of conjugation to antibodies and affordability. Therefore, alkaline phosphatase is one of the most popular enzymes used in ELISA and other immunoassays. On the other hand, previous reports have demonstrated the SPR signal of plasmonic nanoprobe is strongly dependent on the local refractive index.[10] Particularly, AuNRs with large aspect ratios are extremely sensitive to local refractive index variations, thus resulting in a substantial alteration of the SPR signal and hence offer the possibility of constructing ultrasensitive assays. It is expected that even more drastic changes in the local refractive index and consequently the SPR signal will occur if a different metal and in this case silver is coated on the surface of the AuNRs. Moreover, the change in the local refractive index continuously evolves with the advance of the silver coating process.

observed in the presence of  $\text{AgNO}_3$ , alkaline phosphatase, and p-aminophenyl phosphate (Figure 2A). Meanwhile, the colour of the AuNRs solution gradually changed from pale red to green and finally purple in the presence of 0 to 20  $\mu\text{U}$  alkaline phosphatase (Figure 2B). Alkaline phosphatase is an efficient enzyme to catalyze the production of p-aminophenol.[12] More importantly, it was found the SPR signal of the AuNRs remains unchanged in the absence of p-aminophenyl phosphate. Evidently, the observed shift in the SPR signal and the color change are due to the interaction between the AuNRs and the metallic silver produced through the reduction of silver ions by p-aminophenol. It can be clearly seen from the TEM images (Figure 2C, S1) that silver layers exist on the surfaces of the AuNRs after the introduction of alkaline phosphatase after 60 min incubation. In addition, the thickness increased with the increase of alkaline phosphatase concentration. However, a contrary phenomenon occurred when alkaline phosphatase concentration reached  $\geq 30 \text{ pM}$ . Less obvious SPR shift and a new peak at around 400 nm were observed (Figure S2). This is likely due to the fact that the nucleation of free-standing silver particles and the growth of the silver particles occur at high concentrations of reducing agent generated from the high concentrations of alkaline phosphatase (See TEM image in Figure S2). Eventually, instead of the final purple colour, the reaction mixture eventually exhibited yellow colour which is the typical colour of a silver nanoparticle solution. Furthermore, it was also observed that the magnitude of the shift registered by the SPR signal depends on the amount of alkaline phosphatase which in turn on the generated p-aminophenol. The UV-visible spectra of the AuNRs before and after the formation of the AuNR/silver core-shell nanostructures match well with the progression of the deposition on the silver shells on the AuNRs (Figure 2A & C). With the increase of alkaline phosphatase concentration, the magnitude of the SPR shift increased accordingly. It was also noticed that the SPR shift increases with prolonging the incubation time in the cocktail. The  $\Delta\lambda$  versus the concentration of alkaline phosphatase concentration at after 60 min of incubation was plotted in Figure 2D. As seen in Figure 2D,  $\Delta\lambda$  increased gradually with the increasing concentration of alkaline phosphatase. A noticeable SPR shift was already observed even at very low concentrations of alkaline phosphatase, which guarantees the possibility of developing an ultrasensitive ELISA.

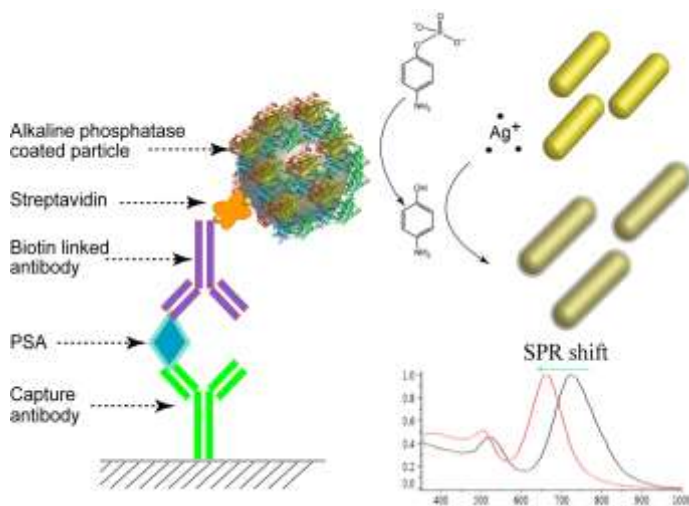


**Figure 1.** Schematic illustration of the working principle of the PSA assay. First, alkaline phosphatase is anchored through a silica nanocarrier by the sandwich structure. Then, alkaline phosphatase catalyses the production of 4-aminophenol. The produced 4-aminophenol, in turn, acts as a reducing agent for the reduction of silver ions and consequent deposition of metallic silver on the AuNRs. As a result, the SPR peak of the AuNRs blue shifted after the AuNRs are coated with silver.

AuNRs with high homogeneity were synthesised following a seed-mediated surfactant-directed approach as previously reported.[11] To facilitate the deposition of the silver shells on the AuNRs, the as-synthesised AuNRs were further purified by one round of centrifugation/redispersion. To confirm the feasibility of signal amplification through the proposed strategy, we first tested whether metallic silver could be preferably deposited on the surface of the AuNRs in the presence of a reducing agent and the deposited silver shells significantly alter the SPR characteristics of the AuNRs. Our results clearly showed that an obvious SPR peak shift is

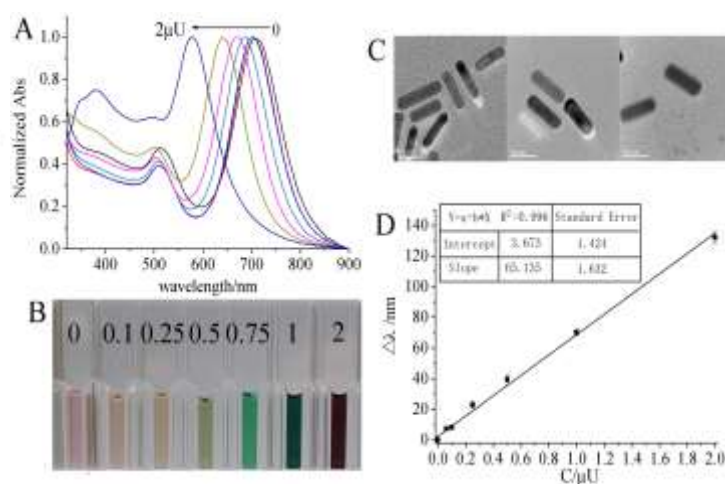


**Figure 2.** (A) The colour change of the AuNRs in different concentrations of alkaline phosphatase; (B) TEM images before and after the enzyme-catalysed deposition of silver (1-3: 0, 0.5, 2  $\mu\text{U}$  alkaline phosphatase); (C) UV-visible absorption spectra of the AuNRs in different concentrations of alkaline phosphatase and (D) the correlation between activity of alkaline phosphatase and the SPR shift of the AuNRs derived from (A).

Having demonstrated the correlation between the SPR signal and the concentration of alkaline phosphatase, we then attempted to apply this signal amplification strategy to PSA immunoassay. By construction the antibody-based sandwich structure, alkaline phosphatase could be introduced into the system through biotin-streptavidin interaction. However, one PSA molecule usually generates only one alkaline phosphatase link point in traditional ELISA. To enhance alkaline phosphatase loading, biotin-modified silica nanoparticles were introduced before enzyme sorption (see Figure 1 and Figure S3). Consequently, streptavidin-conjugated alkaline phosphatase could be loaded onto the silica nanoparticles with high capacity because of their high surface area. Nonetheless, by varying the concentrations of PSA, different quantities of alkaline phosphatase were anchored. Moreover, the cumulative nature of the enzyme-catalysed amplification strategy via silver deposition offered a highly flexible means to significantly improve the sensitivity of the assay at will. To maximise the sensitivity, lower the cost and have a reasonable turnaround time, it was found that a period of 60 min incubation with 5 mM p-aminophenyl phosphate is sufficient for the detection of PSA down to fg/ml levels.

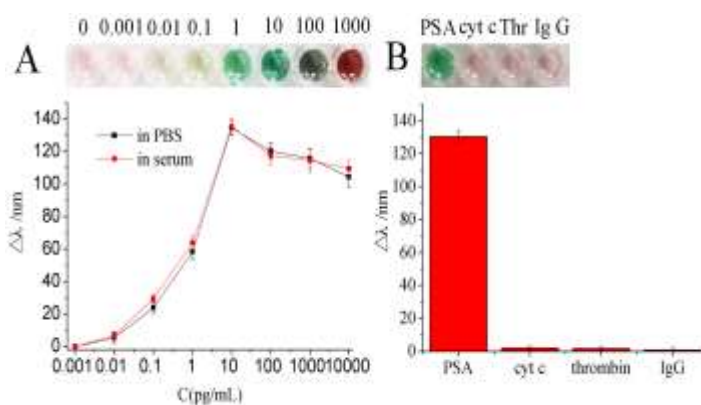


**Figure 3.** (A) SPR shift of the AuNRs at different concentrations of PSA in PBS and serum; insert picture shows the colours of the AuNRs in the presence of 0, 0.001, 0.01, 0.1, 1, 10, 100 and 1000 pg/mL PSA, respectively. (B) the SPR shifts of the AuNRs in the presence of 10 pg/mL PSA and 10 ng/mL cyt c, thrombin and IgG, respectively. Insert picture shows the colours of the AuNRs in the presence of PSA, cyt c, thrombin and IgG, respectively.

As shown in Figure 3A, the colour of the AuNR solution changed from pale red to green, purple and brown with the increase of PSA concentration from 0 to 1.0 ng/ml, which can be easily differentiated by the naked eye. This obvious colour change provides a convenient and instrument-free means for the readout of PSA assay. Initially, the SPR shift increased with increasing PSA concentration in the range of 10 fg/ml–10 pg/ml, reached a maximum at 10 pg/ml and then decreased with a further increase in PSA concentration. When the concentration of PSA was lower than 10 pg/ml, the silver coatings on the AuNRs played a dominant role since continuous incubation in AgNO<sub>3</sub> resulted in the increase in the coverage and eventually the thickness of the silver layer on the surface of the AuNRs, thus enhancing the SPR shift. Nevertheless, nucleation and growth of independent silver nanoparticles became evident with extremely high concentrations of PSA e.g. 20 pg/ml and beyond. The lowest concentration of PSA where the colour change can be unambiguously distinguished by the naked eye was 100 fg/mL. By measuring the SPR spectra of each sample, we observed that the SPR peak blue-shifted with the increase of PSA concentration which is consistent with the colour change. In addition, 10 fg/mL PSA was

successfully detected colourimetrically. To validate the specificity of the assay, three other proteins, namely thrombin, human immunoglobulin G (IgG) and cytochrome C (cyt C), were tested. As shown in Figure 3B, 10 pg/ml PSA led to an SPR shift as large as 130 nm, whereas 10 ng/ml other proteins exhibited no observable SPR shifts. Similar results were obtained when the same experiments were conducted in serum. In terms of the blank sample, the solution remained pale red because neither capture antibody nor the biotin linked antibody can specifically interact with any of the constituents of serum, thus demonstrating that matrix of clinical samples has negligible effects on the assay. This result makes this assay very appealing for the detection of PSA in real clinical samples. Therefore, conclusion could be reached that the colour change of the solution and the SPR shift are based on the specific immunoreaction between PSA and its antibodies, rather than the nonspecific interactions. Furthermore, we tested the same PSA solutions with a commercial horseradish peroxidase (HRP)-based ELISA, which is the most commonly used colorimetric assay for PSA (Figure S4). The lowest detectable concentration for PSA using our colorimetric method was compared with that of the HRP-based ELISA. The detection limit of the HRP-based ELISA was found to be 100 pg/mL, which is four orders of magnitude higher than that of our AuNR-based PSA assay. This naked-eye detection becomes particularly useful in resource-constrained areas where complex instrument is not available. The detection limit of the present AuNR-based plasmonic immunoassay, which was in the low fg/ml range, was more sensitive or comparable to other nanoparticle-amplified immunoassays (Table S1).

In conclusion, a plasmonic signal amplification method has been developed that allows for highly sensitive and selective detection of proteins. This facial signal amplification strategy is based on the alkaline phosphatase induced coating of ultrathin silver layers on the AuNRs. Consequently, the SPR peak blue-shifted accompanied by a colour change due to the drastic alteration of local refractive index. For the detection for PSA, the immunoassay incorporated with the proposed amplification strategy exhibited significant advantage over conventional ELISA for the same analyte in terms of simplicity, stability and sensitivity. As low as 10 fg/mL PSA can be detected using the proposed assay, which is four orders of magnitude better than that of conventional ELISA. This signal amplification strategy can be easily extended to the detection of other analytes where alkaline phosphatase is engaged as an enzyme label, thus implying that the AuNR-based plasmonic amplification method can be adopted as a universal amplification method in immunoassays and many other plasmonic assays.

We thank Ministry of Education (Grant No: R-143-00-588-112) and the Agency for Science, Technology and Research (Grant No: 1222703071) for their financial support.

## Notes and references

Department of Chemistry, National University of Singapore, 3 Science Drive 3, Singapore 117543, Republic of Singapore.

† Electronic Supplementary Information (ESI) available: Experimental details, additional characterization of the AuNR-based amplification method. See DOI: 10.1039/c000000x/

- (a) J. Kirsch, C. Siltanen, Q. Zhou, A. Revzin, A. Simonian. *Chem. Soc. Rev.* 2013, **42**, 8733-8768; (b) J. J. Xu, W. W. Zhao, S. Song, C. Fan, H. Y. Chen. *Chem. Soc. Rev.* 2014, **43**, 1601-1611.

- 2 J. Shen, Y. Li, H. Gu, F. Xia, X. Zuo. *Chem. Rev.* 2014, **114**, 7631-7677.
- 3 M. H. Black M. Giai, R. Ponzzone, P. Sismondi, H. Yu, E.P. Diamandis, *Clin. Cancer Res.* 2002, **6**, 467-473.
- 4 S. Radowicki, M. Kunicki, E. Bandurska-Stankiewicz, *Eur. J. Obstet. Gynecol. Reprod. Biol.* 2008, **138**, 212-216.
- 5 P. D. Howes, S. Rana, M. M. Stevens, *Chem. Soc. Rev.* 2014, **43**, 3835-3853.
- 6 O. Hess, J. B. Pendry, S. A. Maier, R. F. Oulton, J. M. Hamm, K. L. Tsakmakidis, *Nat. Mater.* 2012, **11**, 573-584; (b) J. N. Anker, W. P. Hall, O. Lyandres, N. C. Shah, J. Zhao, R. P. Van Duyne, *Nat. Mater.* 2008, **7**, 442-453; (c) H. He, X. Xu, H. Wu, Y. Jin, *Adv. Mater.* 2012, **24**, 1736-1740; (d) R. de la Rica, M. M. Stevens, *Nat. Nanotechnol.* 2012, **7**, 821-824; (e) L. Rodríguez-Lorenzo, R. de la Rica, R. A. Álvarez-Puebla, L. M. Liz-Marzán, M. M. Stevens, *Nat. Mater.* 2012, **11**, 604-607; (f) H. J. Wu, J. Henzie, W. C. Lin, C. Rhodes, Z. Li, E. Sartorel, J. Thormer, P. Yang, J. T. Groves, *Nat. Methods.* 2012, **9**, 1189-1191.
- 7 K.M. Mayer, J. H. Hafner. *Chem. Rev.* 2011, **111**, 3828-57.
- 8 H. Chen, L. Shao, Q. Li, J. Wang, *Chem. Soc. Rev.* 2013, **42**, 2679-2724.
- 9 M. E. Nasir, W. Dickson, G. A. Wurtz, W. P. Wardley, A. V. Zayats, *Adv. Mater.* 2014, **26**, 3532-3537; (b) W. Ni, Z. Yang, H. Chen, L. Li, J. Wang, *J. Am. Chem. Soc.* 2008, **130**, 6692-6693; (c) L. Chen, B. Wu, L. Guo, R. Tey, Y. Huang, D. H. Kim, *Chem. Commun.* 2014, **51**, 1326-1329.
- 10 N. E. Motl, A. F. Smith, C. J. DeSantisa, S. E. Skrabalak, *Chem. Soc. Rev.* 2014, **43**, 3823-3834.
- 11 X. Yang, X. Liu, Z. Liu, F. Pu, J. Ren, X. Qu, *Adv. Mater.* 2012, **24**, 2890-2895.
- 12 Willner, R. Baron, B. Willner, *Adv. Mater.* 2006, **18**, 1109-1120.